Advanced Drug Delivery Reviews 69-70 (2014) 217–224

Contents lists available at ScienceDirect

Advanced Drug Delivery Reviews

journal homepage: www.elsevier.com/locate/addr

In vitro microbial culture models and their application in drug development☆

Saurabh Vyawahare [a], Qiucen Zhang [b], Alexandra Lau [c], Robert H. Austin [d,*]

[a] Princeton Institute for the Science and Technology of Materials, Princeton University, Princeton, NJ 08544, USA
[b] Department of Physics, University of Illinois at Urbana–Champaign, Urbana, IL 61801, USA
[c] Department of Physics, Mount Holyoke College, South Hadley, MA 01075, USA
[d] Department of Physics, Princeton University, Princeton, NJ 08544, USA

ARTICLE INFO

Available online 21 February 2014

Keywords:
Antibiotics
Resistance
Evolution
Microbes
Microfluidics

ABSTRACT

Drug development faces its nemesis in the form of drug resistance. The rate of bacterial resistance to antibiotics, or tumor resistance to chemotherapy decisively depends on the surrounding heterogeneous tissue. However, in vitro drug testing is almost exclusively done in well stirred, homogeneous environments. Recent advancements in microfluidics and microfabrication introduce opportunities to develop in vitro culture models that mimic the complex in vivo tissue environment. In this review, we will first discuss the design principles underlying such models. Then we will demonstrate two types of microfluidic devices that combine stressor gradients, cell motility, large population of competing/cooperative cells and time varying dosage of drugs. By incorporating ideas from how natural selection and evolution move drug resistance forward, we show that drug resistance can occur at much greater rates than in well-stirred environments. Finally, we will discuss the future direction of in vitro microbial culture models and how to extend the lessons learned from microbial systems to eukaryotic cells.

© 2014 Elsevier B.V. All rights reserved.

Contents

1. Introduction

The emergence of antibiotic resistance in bacteria remains a persistent problem worldwide [1]. Previous studies isolated and characterized various resistant mutants, which provided valuable insights into the biological processes that are altered in mutant bacteria [2–4]. But the rate of evolution of antibiotic resistance is still unclear, especially in an environment that bacteria naturally live. Understanding the rate of evolution is crucial for developing new antibiotics and planning effective treatments.

Microfluidics is the science and technology of systems that process or manipulate small (10^{-9} to 0^{-18} l) amounts of fluids [5,6]. Microfluidics provides a reproducible and controllable way to reconstruct various important factors of in vivo environments, which is challenging to achieve via conventional test tubes [5,7,8]. Two major types

☆ This review is part of the *Advanced Drug Delivery Reviews* theme issue on "Innovative tissue models for drug discovery and development".

* Corresponding author. Tel.: +1 609 258 4353; fax: +1 609 258 1115.
E-mail address: austin@Princeton.EDU (R.H. Austin).

http://dx.doi.org/10.1016/j.addr.2014.02.005
0169-409X/© 2014 Elsevier B.V. All rights reserved.

of control have been realized in microfluidic devices. One is controlling the reaction inside the device via the laws of fluids at the small scale. Our group pioneered this approach by demonstrating rapid mixing in a hydrodynamic focusing device [9] and further added additional passive controls by creating regular structures on silicon wafers [10–13]. The other approach of the control is to make on-chip active components — valves [14–16], mixers [17–19] and pumps [20,21]. Using active or passive control, many methods to culture bacteria in microfluidic systems have been published [22–26,7], including recent microfluidic devices to mimic bacterial growth in human tissue [27,28].

When members of a bacterial community are allowed to interact with complex environments, dramatic changes in the pace of evolution and selection have been seen in both experiments and simulations [29–33]. Specifically, ecological conditions like drug gradients and the presence of small population niches can induce rapid drug resistance [34,35,10]. Thus, full understanding of the nature of drug resistance requires controlling these ecological conditions along with cell culture. Here, we will review two main types of microfluidic devices recently developed as in vitro microbial culture models combined with ecologies. We will highlight the key results got from experiments performed by combining these new devices with other technologies in genomics such as next generation sequencing and DNA microarray. Finally, we will provide an outlook on two aspects: one is the advancement of in vitro microbial culture models in the future, particularly how microfluidic devices can be integrated with various genomics analysis tools as a unified platform to assess the development of drug resistance in a high-throughput and systematical fashion; the other is how to apply knowledge learned from microbial systems to eukaryotic systems, where both opportunities and challenges will be discussed.

As an aside, applications of microfluidics to drug development have been well reviewed [36,37], and in particular, there have been many rapid developments in using droplet based approaches for economically useful mutants [38]. We refer the reader interested in drug development to those reviews and papers. In this review we shall only focus on the coming together of cell culture and ecological niches to influence drug resistance in microfluidic devices.

2. Wright's evolution principle

The design principles of the new generation of in vitro microbial culture models came from Wright's seminal contributions concerning the importance of the number of cells n_i in a particular microhabitat i [39,40]. The number n_i of individuals within a particular microenvironment niche strongly influences the outcome of natural selection on the fixation probabilities $P(n_i,s_i)$ and fixation times $\tau(n_i,s_i)$ within that particular microhabitat. Suppose that in a population of n_i cells, a mutation appears in an individual with a relative fitness advantage s_i over the other $n_i - 1$ competitors. The probability due to genetic drift for the eventual fixation of that mutation in all the n_i individuals scales as:

$$P(n_i,s_i) = \frac{1-exp^{-2s_i}}{1-exp^{-2n_i s_i}} \quad (1)$$

while the mean time to fixation scales as:

$$\tau(n_i,s_i) \sim \frac{1}{s_i} ln(n_i). \quad (2)$$

Eqs. (1) and (2) have some interesting implications. First, note the explicit dependence on the number of competing individuals n_i, so that the probability of fixation is dependent on the product of the fitness s_i and the number of competitors $n_i - 1$. In a large population, which means that $s_i n_i \gg 1$, the most fit clone *always* wins and fixes the mutation. However, if $s_i n_i \leq 1$, it is entirely possible for less fit clones to fix, even clones with negative fitness! Fig. 1 shows the dependence of the probability of fixation on population number n_i and relative fitness s_i. This is an important point: what really matters in fixation probabilities is the product of fitness times population number. Of course, this formula is just for genetic drift in a population and does not describe true evolution which involves both the generation of mutations and the process of natural selection, but it should give some idea of the role that population size plays in the role of gene fixation. Similarly, the time to fixation also depends on the number of competitors: the larger n_i is, the longer it takes to fix.

Within a complex ecology such as a biofilm we can expect that there is spatial and temporal heterogeneities in the fitness s_i and number n_i as long as there is an initial mutagenic aspect to the cell reproduction. Also, because of the complexity of a biofilm or bacteria within the tissue, there will be very strong gradients in drug delivery, with a corresponding distribution in the probabilities of fixation and time to fix for mutants which show the phenotype of resistance.

Little is known about the influence of the steepness of fitness gradients on the rates of evolutionary adaptation to stress, but we can guess a few things. First, recall from Eq. (1) that the smaller the number of cells at a given fitness advantage, the more likely fixation is to occur. On the other hand, there is also the phenomenon of Muller's Ratchet [41], which is that the smaller the population, the more likely it is for lower fitness mutants to fix, if there is no exchange from other populations. Thus, it is difficult at present to truly predict what is the optimum drug dose without detailed knowledge of the drug gradients, metapopulation sizes and motility between local populations. However, if these can be measured then a true theory of evolution of drug resistance evolution rates is within reach.

3. Microfluidic devices implementing spatial drug gradients

3.1. Rapid evolution in microfluidic devices

Our fundamental point concerning the inevitable emergence of resistance to a mutagenic stressor under the appropriate ecological and metapopulation parameters can be shown by designing using microfabrication techniques designed to quantitatively test these ideas. We have done a fundamental experiment which shows the power of these ideas [10]. The design and characterization of the devices are shown in Fig. 2.

We used *Escherichia coli* bacteria and the highly mutagenic bacteriastatic antibiotic ciprofloxacin. Ciprofloxacin is a member of the quinolone family of antibiotics and functions by binding to DNA gyrase [42]. Ciprofloxacin traps the gyrase–DNA complex at the state when the DNA is cut, thereby inhibiting DNA replication and cell division, in essence preventing the cell from dividing but not killing the cell (i.e., it is cytostatic, not cytotoxic). The generation of single-stranded DNA by stalled ciprofloxacin-bound gyrase is known to trigger, via the self-cleavage of the repressor LexA, removal of LexA from transcription factor sites. Removal of LexA activates the transcription error-prone DNA polymerases [43]. The effective mutagenic rate u^* due to the SOS response is 10^{-5} mutants/viable cell/day, 10,000 times greater than the base rate u [44].

Fig. 3 shows the emergence of resistance from wild-type *E. coli* over 20 h. When bacteria are inoculated into the center of the device, chemotaxis due to consumption of nutrients at low flow rates quickly drives them to the perimeter of the device. At the Goldilocks point (gold arrow, Fig. 3(A)) there is a combination of high population gradient and high mutation rates. In this experiment the concentration of ciprofloxacin flowing along the bottom side of the device is 10 μg/mL, approximately 200 times the minimum inhibitory concentration of ciprofloxacin. Yet, as Fig. 3 shows there is ignition of resistance at the Goldilocks point and subsequent rapid movement of resistant bacteria around the periphery of the device and invasion back to the center in 20 h.

The basic reason for this invasion of resistance is the fitness advantage for mutant resistant *E. coli* in a micro-environment where the

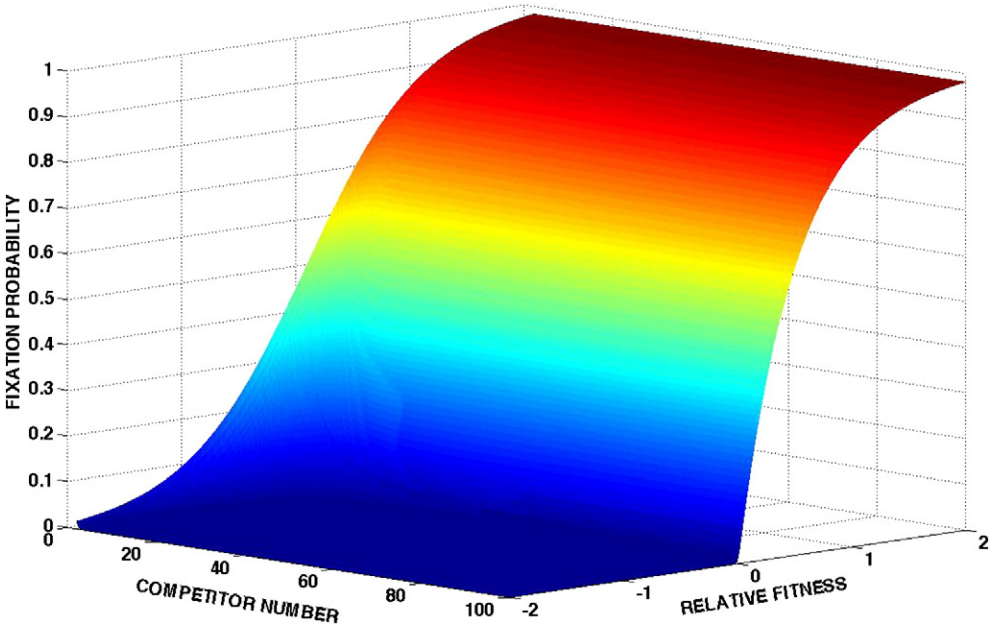

Fig. 1. Fixation probability of a single mutation with relative fitness advantage *s* as a function of competitor number *n* and relative fitness advantage *s*.

food reservoir is nearby and no other sensitive competitors can live. Since the device is composed of small micro-habitat patches, the resistant *E. coli* can rapidly fix in these small populations. Fig. 3(D) to (F) shows growth of resistant mutant bacteria upon re-inoculation in a new chip with the same culture conditions as in Fig. 3(A) to (C).

The genetic analysis of the evolution of antibiotic resistance in these complex ecologies was astounding. Four apparently functional SNPs were identified at the end of the experiment. A detailed understanding of the order in which the SNPs occur is essential. It is unlikely that the four SNPs emerged simultaneously; in all likelihood they are sequential. The new question then is, are there any fundamental mechanisms that drive the sequential emergence of mutations?

3.2. The logic of gene placement

We determined using Comparative Genomic Hybridization (CGH) [45] that the most rapid genomic change occurring, within 1 h after exposure to ciprofloxacin, is copy number changes (gains/losses) in the DNA content, changes which are correlated with the position of genes on the *E. coli* chromosome. *E. coli* cells were grown in LB broth. While in the exponential growth phase, the appropriate antibiotic (ciprofloxacin, chloramphenicol or kanamycin) was added for a specified period of time, followed by genomic DNA extraction.

The DNA was purified and labeled with Cy3 (wild type) or Cy5 (antibiotic exposed). The labeled DNA from the wild type and antibiotic

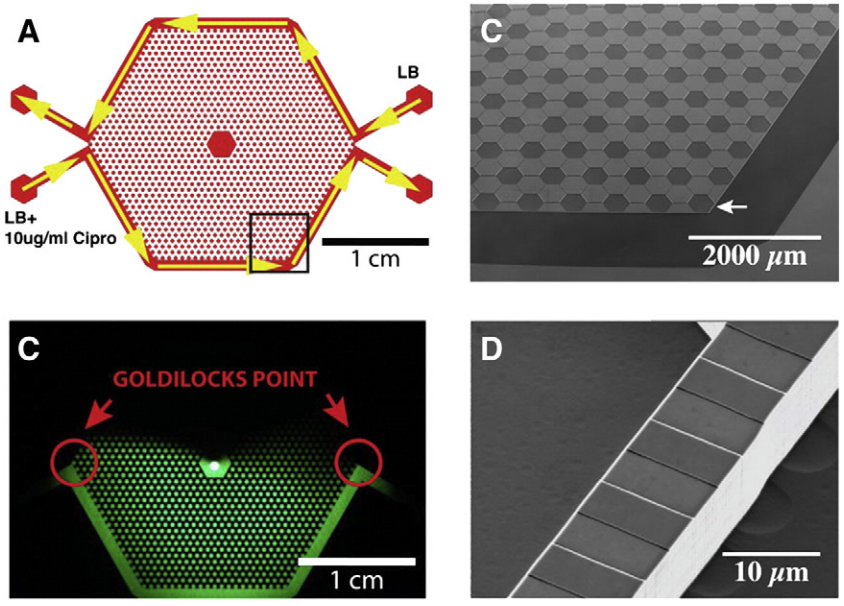

Fig. 2. (A) An overview of the entire micro-ecology, showing the flow of the nutrient streams and the nutrient + drug containing streams. The nutrient stream is ×1 LB broth, while the nutrient + ciprofloxacin stream is ×1 LB broth + 10 μg/mL ciprofloxacin. (B) Image of the expected drug concentration. (C) Scanning electron microscope (SEM) image of the area of the array in (A) outlined by the box. (D) SEM image of the nanoslits at the micro-ecology periphery. The nanoslits are etched down 100 nm and are 6 μm wide and 10 μm long.

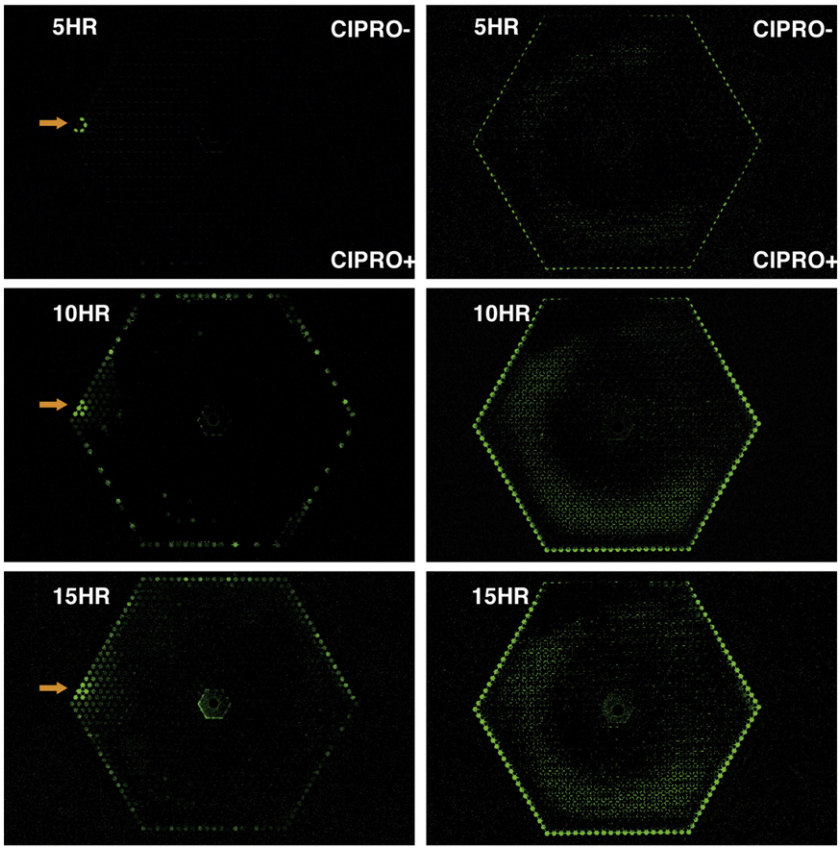

Fig. 3. (A to C) Initial inoculations of 10^6 wild-type bacteria with ciprofloxacin (10 mg/mL) in the bottom channel. (A) Emergence of resistance to ciprofloxacin 5 h after inoculation. The Goldilocks microenvironment is shown by the orange arrow. (B) Spread of resistant bacteria around the periphery of the microenvironments at 10 h after inoculation. (C) Continued growth of ciprofloxacin resistant bacteria after 15 h. (D to F) Growth of resistant mutant bacteria upon re-inoculation in a new chip with the same culture conditions as in (A) to (C).

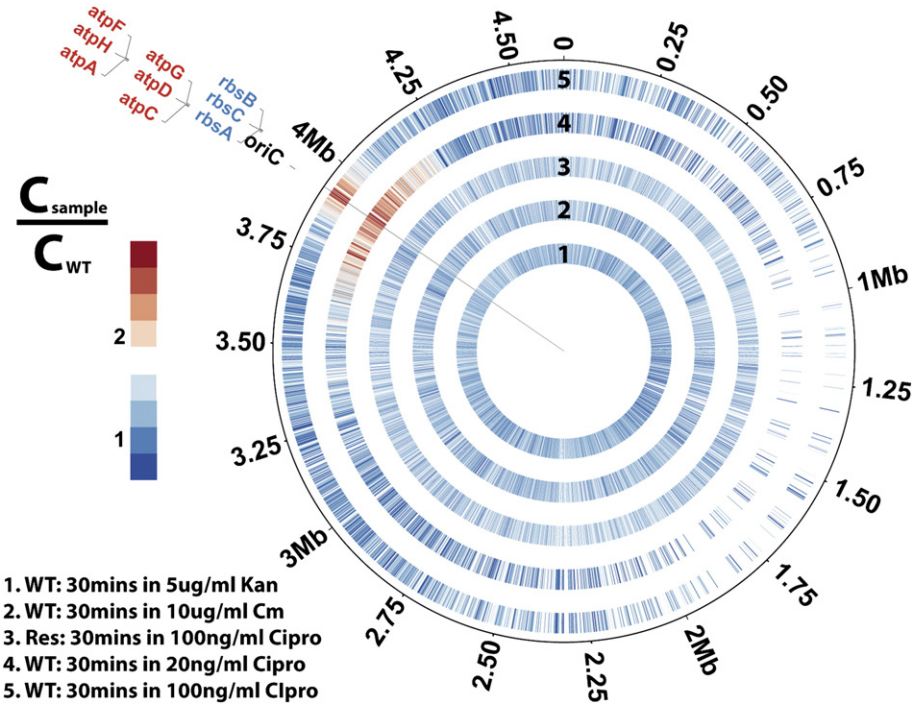

Fig. 4. DNA copy number changes are plotted by Circos [48]. Track 1 represents wild-type E. coli treated by 5 μg/mL kanamycin for 30 min, Track 2 represents wild-type *E. coli* treated by 10 μg/mL chloramphenicol for 30 min, Track 3 represents ciprofloxacin resistant *E. coli* treated by 100 ng/mL ciprofloxacin for 30 min, Track 4 represents wild-type *E. coli* treated by 20 ng/mL ciprofloxacin for 30 min, Track 5 represents wild-type *E. coli* treated by 100 ng/mL ciprofloxacin for 30 min.

exposed *E. coli* was hybridized on a custom *E. coli* array (Agilent, CA). The array contains 8 lanes of 15,744 spots. Each spot is printed with 60 base probes. Beside all the control spots, there are two major groups of probes: one is 10,014 tilling probes which tile the entire 4.6 million base-pair *E. coli* genome, the other group includes probes complementary to the 4287 known *E. coli* genes.

After hybridization and wash steps, the microarray is scanned using a GenePix 4200A microarray scanner. Fig. 4 summarizes the results of CGH experiments where *E. coli* were challenged with three different antibiotics: (1) ciprofloxacin (2) kanamycin, an antibiotic which interacts with the 30S subunit of prokaryotic ribosomes and so induces mistranslation but does not affect DNA replication [46], and (3) chloramphenicol, an inhibitor of protein chain elongation and thus also not a blocker of DNA replication [47].

Since the data set is normalized both with respect to the amount of DNA as well as relative to that of wild type *E. coli*, it should be noted that only changes that differ from the wild-type will appear in the signal. So for instance, if the entire chromosome was amplified with respect to the wild type *E. coli*, this will not result in a signal, but a difference in one region compared to another (relative to that in the wild type) will show up as a signal. Each small radial line in Fig. 4 represents a probe which has been filtered to remove any artifacts of micro-array printing.

There is a clear increase in gene copy number observed around the *oriC* when wild-type *E. coli* are challenged by ciprofloxacin. Such amplification of the gene copy number near *oriC* depends on the concentration of ciprofloxacin, and becomes more tightly constrained around the *oriC* as the concentration of ciprofloxacin increases, as seen in track 4 and track 5 of Fig. 4. This is probably because more replication forks are stalled at higher concentrations of ciprofloxacin. In contrast, there are no obvious gene copy number changes in ciprofloxacin resistant *E. coli* after the same exposure to ciprofloxacin, because it has already evolved resistance to the stress. Note that multiple copy generation is not seen for non-genotoxic antibiotics such as chloramphenicol and kanamycin (tracks 1 and 2 in Fig. 4) which do not initiate the SOS response.

Since replication is stalled by the interaction of gyrase A with ciprofloxacin, even at the presumably lower ciprofloxacin concentrations within the bacterium the progression of DNA polymerases around the chromosome from the *oriC* is presumably spatially exponentially damped by the replication forks. We would then expect that the critical efflux pump genes would be clustered around the *oriC* of *E. coli* so that as the first line of defense they would be the ones most likely to be expressed.

Indeed we see that the transporter associated genes are clustered around the *oriC* as shown in Fig. 4. The gene copy number variation possibly serves as a critical driving force of the rapid evolution, because first, changes in copy number could change the transcription levels of genes included in the regions of variable copy number [49]; second, redundant copies of genes also allow some copies to evolve new or modified functions while other copies maintain the original function [50]. In contrast to several active mechanisms that have been proposed as causes of copy number variation [49], gene placement with respect to the *oriC* provides a passive and natural way to preferentially increase the copy number of certain efflux pump genes, which helps the bacteria to pass the initial hurdle under stress.

3.3. Time dependence of drug recovery

The time dynamics of the increase in copy number during exposure to ciprofloxacin and the decay of the copy numbers after removal of the antibiotic reveal the dramatic ways that the bacterial genome is dynamically sculpted under stress and the fascinating dynamics of removal of the copy numbers when the stress is removed. To measure the time dependence of the increases in gene copy number with time, the concentration of ciprofloxacin was fixed at 20 ng/mL and bacteria were sampled at 15, 30, and 60 min using CGH against wild-type cell without any drug exposure.

While the copy number induced by cipro stress shows a basic independence to the duration of the cipro exposure, this is not true for the dynamics of the removal of the copy numbers when the stress is removed. *E. coli* cells grown in LB broth were exposed to antibiotic cipro at a concentration of 20 ng/mL. After cipro exposure for a predetermined time, cells were centrifuged and resuspended in plain LB broth without any antibiotic. Samples were removed every 15 min from this mixture.

From these samples, genomic DNA was extracted and real time PCR was performed on two genes: gyrA and rbsA. gyrA and rbsA were chosen for this experiment based on our previously published work that showed point mutations in these two genes leading to cipro resistance [10], and also because the two genes are located at the opposite ends of the circular *E. coli* genomic DNA.

The concentration of DNA extracted from the samples was measured using a spectrometer to ensure that each well in the plate had approximately 8 ng of genomic DNA. From the PCR curves Ct valves were extracted and the difference in Ct number for the two genes was compared. The real time PCR was repeated four times (2 biological replicates, done twice) and error bars calculated from the standard deviation. Two primers were designed for the RT-PCR: a control for gyrA, the target of ciprofloxacin and the other for rbsA, the D-ribose transporter near the *oriC*. The gyrA was included as a negative control baseline since the CGR did not show any significant changes in the copy numbers of gyrA during the cipro exposure. Bacteria which had been exposed to 20 ng/mL of cipro for varying durations were resuspended in LB broth and then assayed using RT-PCR for copy numbers of rbsA. Three periods of exposure to cipro were studied: 60 min, 120 min and 240 min.

Fig. 5 shows the surprising results of the RT-PCR: the rate at which multiple copies of the rbsA gene are removed is a function of the duration of the exposure, that is return back to the wild-type genome is a non-linear function of the duration of exposure to stress. Bacteria exposed to 60 min of cipro lost the extra copies with a time constant $\tau_{1/2}$ of approximately 50 min, however bacteria exposed to cipro for 120 min had a $\tau_{1/2}$ of approximately 130 min, and bacteria exposed to 130 min, and bacteria exposed for 240 min had an extrapolated $\tau_{1/2}$ of approximately 500 min.

The placement of the genes on the *E. coli* genome from the *oriC* is not random but instead is critical; first for the creation of a mesoscopic ecological niche, and then the emergence of resistance from this niche. Removal of the stress reverses the evolution of the response, but in a way that indicates that the bacteria adjust devolution rates as a function of the duration of the prior stress. Knowledge of the duration-dependent rates is critical for developing time-dependent schemes for decreasing the evolution of drug resistance in antibiotic and chemotherapy treatments.

4. Microfluidic devices implementing temporal drug variations

To study time dependent dosage, we have designed another type of microfluidic device. In this device, cells are free to move but only inside a certain amount of space so that we can trace individual cell for a long time. These devices are variants of the mother-machine design [51]. Fig. 6 illustrates the microfluidic culture device. These devices were made using standard soft lithography techniques using PDMS as the elastomer. Briefly, we use SU8 and SPR 220-7 photoresists to form side and main channels respectively on a silicon wafer. This is followed by soft-lithography with PDMS elastomer.

The width and depth of the central channels and side channels can be varied to suit the bacteria and experiments performed. For channels with a large width to height ratio the channels may collapse — in this case we use an off ratio (1:5 instead of 1:10) PDMS curing agent:polymer mix to have more stiff walls that don't collapse. In the latest versions of these devices on multi-layer soft-lithography can be used to

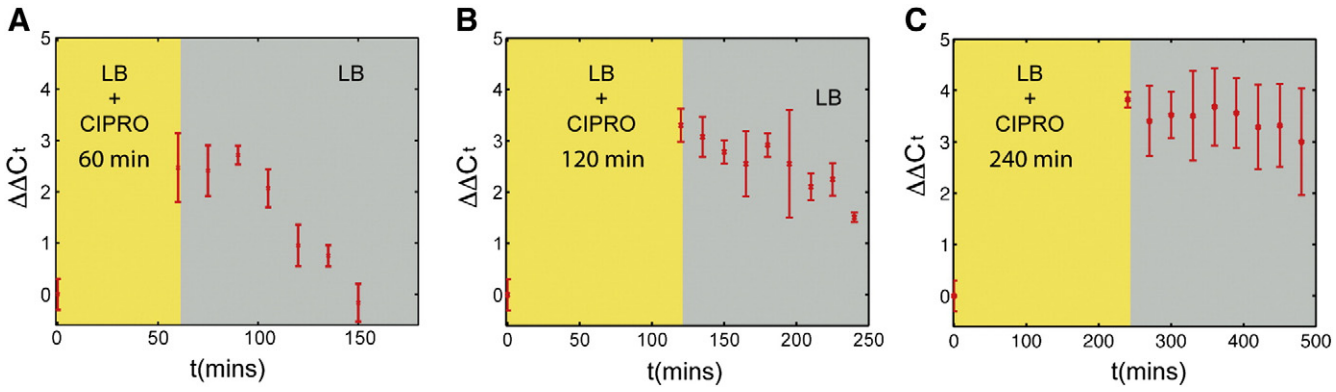

Fig. 5. Removal of stress-induced multiple gene copies as a function of the duration of the exposure to cipro.

make elastomeric valves to direct media and drugs. The PDMS chip is cured, and cut, and inlet and outlet ports are cored and finally bonded to a #1.5 cover glass via plasma bonding.

Cells are introduced through the main channel. They explore the space, and using a combination of pressure and backfilling they can be introduced to the side-channels where some of them get stuck. The height of the channels ensures that only a single layer of bacteria can comfortably fit. The media and drugs are then flown in through the central channels using syringe pumps. This flushes away any bacteria not in the side channels. Diffusion ensures that the side channels are well mixed in a matter of minutes (side channels must be free of debris), and imaging experiments can be performed over a period of several hours or more.

The difference between these devices and the silicon ones previously described is that in this case PDMS/glass being a transparent substrate allows the use of high numerical aperture objectives that can be placed closed to the cover glass, along with illumination from the other side, allowing for example phase contrast imaging. Thus single cells can be followed over a long period of time. Another difference is that PDMS is gas permeable unlike silicon. Depending on the type of experiment

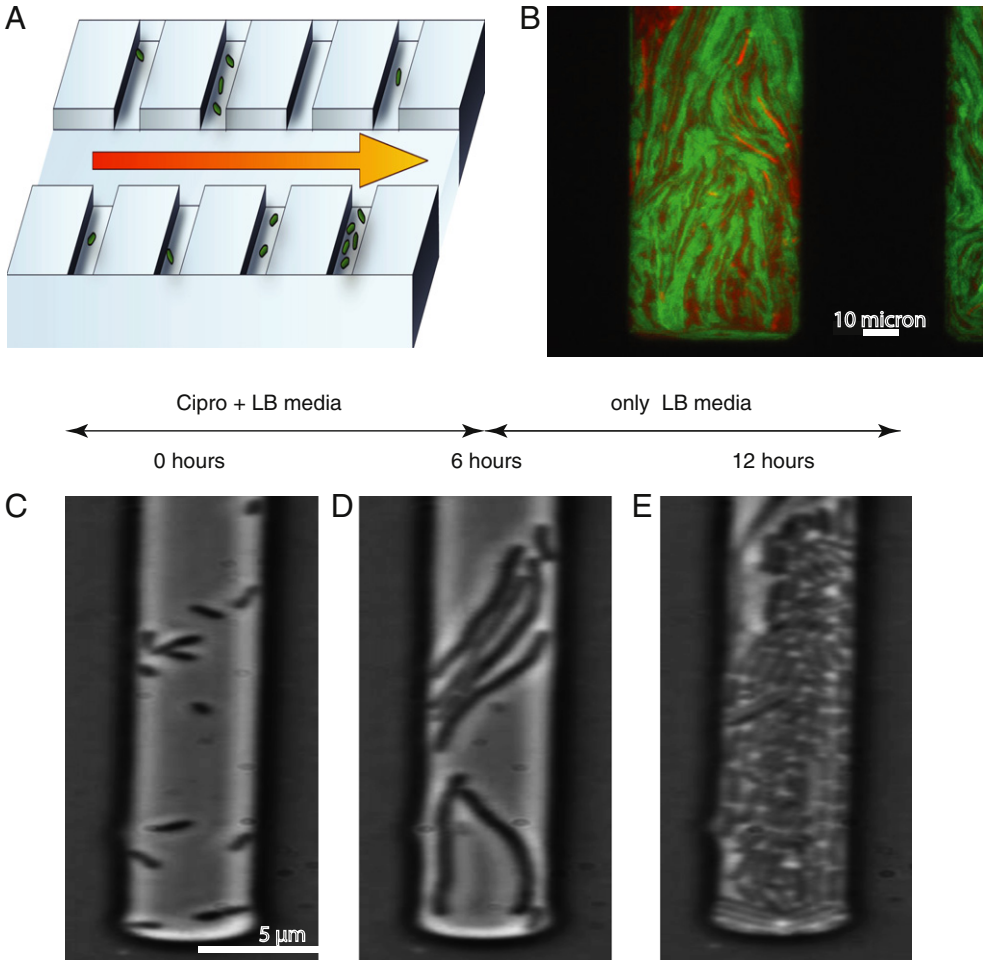

Fig. 6. (A) Microfluidic device for single cell time lapse imaging under antibiotic stress shown in schematic diagram (not to scale) consists of a wide central channel and narrower side channels where bacteria are trapped; (B) *E. coli* with GFP and RFP fluorescence markers form dense biofilms after one day of cipro exposure; (C), (D), and (E) Examples of a time-dependent dosage experiment where cells were exposed to drug for 6 h followed by plain LB media. Cell filaments on antibiotic exposure and then recover.

being performed this feature can be an advantage or a hindrance. For instance channels that have a dead end can still be easily filled, but it is possible for cells to communicate between nearby chambers via gaseous factors like hydrogen peroxide which can complicate analysis of experiments.

As shown in Fig. 6, it is easy to change the media in the central channel and do time dependent experiments. Understanding the effect of time varying drug dosage as we showed earlier is of great importance. Newer type of therapies – where drugs are given in smaller concentrations but often — metronomic therapy – can be explored in such devices.

5. Outlook

Our central premise is that to understand drug resistance it is not sufficient to perform experiments in well stirred, homogeneous environments. As we have showed, these types of experiments are likely to miss important details. Further it is important to be able to continuously observe cells while they interact with drugs. Newer microfluidic devices will allow us to study both cells in spatially and temporally heterogeneous environments, imaging them at the single cell level while drug dosage is varied.

However, the phase space to explore is large — and single experiments will not do. Several questions still need to be answered: for instance what should be the drug concentrations on the boundaries of the gradient, what should be the initial population densities? We already know from our previous work that initial population densities do matter: the emergence rate of resistance and that the spatial patterns of this emergence change, but that is for the same fixed initial drug concentration of $\times 200$ the cipro MIC. What if we change that? In which direction should we change it? We are afraid that the only way we see to do this is simply to carry out many simultaneous experiments with many different initial drug concentrations at the boundaries and map out the evolution dynamics. Technical innovations are needed to increase our ability to do many experiments in parallel.

One recent technical innovation we have made now is the fabrication of a 100 mm silicon wafer that holds 4 independent experiments simultaneously. To achieve an even greater parallelization we would need to use robotic systems. An example is a large-scale multiple incubator system developed by Professor Ted Cox at Princeton University, originally for looking at clonal population variations in *Dictyostelium* [52]. Fig. 7 shows the "small" version of device that we will use for the initial version of this massively parallel experiment. It can do 100 evolution experiments simultaneously. The "large" version of this device, which does exist, has an area $\times 10$ that of the smaller one, it could do $\times 1000$ drug experiments simultaneously!

Besides bacteria it is possible to do similar experiments in eukaryotic cells — robust, fast growing cells like yeast present no problems, but mammalian cells are more difficult due to the longer doubling times (days rather than hours) and the need for control of gas concentrations and humidity. The ecologies must also be larger in size to accommodate the larger cells — the volume of an average bacterial cell is three orders of magnitude smaller than that of a mammalian cell. Gas exchange especially poses challenges in experiments with silicon devices. Silicon based microfluidic ecologies are sealed with glass slides which are impermeable to air, and the structures are etched out of silicon, which is equally impermeable. Nevertheless, with any material choice, many ways to culture eukaryotic cells are available [53,54] and some preliminary experiments in this direction with cancer cell lines have been attempted by us with encouraging results [55]. Combining bacterial and eukaryotic cell cultures in one chip also represents a promising area of work [56].

The devices and data we have described here offer a template for exploring the rates at which antibiotic resistance arises in the complex fitness landscapes that prevail in vivo. Furthermore, we believe the bacterial work provides a framework for exploring rapid evolution in complex contexts such as cancer [57].

Acknowledgment

The authors wish to thank Donna Storton, Jessica Buckles, John Matese and Laurie Kramer at the Lewis-Sigler Institute Microarray Facility, Princeton University. This work was supported by NSF grant NSF0750323 and National Cancer Institute grant U54CA143803. AL was supported by NSF REU in Molecular Biophysics. The content is solely the responsibility of the authors and does not necessarily represent the official views of the National Cancer Institute or the National Institutes of Health.

References

[1] S. Levy, B. Marshall, Antibacterial resistance worldwide: causes, challenges and responses, Nat. Med. 10 (2004) S122–S129.
[2] I. Bjedov, O. Tenaillon, B. Gerard, V. Souza, E. Denamur, M. Radman, F. Taddei, I. Matic, Stress-induced mutagenesis in bacteria, Science 300 (2003) 1404–1409.
[3] V.M. D'Costa, K.M. McGrann, D.W. Hughes, G.D. Wright, Sampling the antibiotic resistome, Science 311 (2006) 374–377.
[4] M.O. Sommer, G. Dantas, G.M. Church, Functional characterization of the antibiotic resistance reservoir in the human microflora, Science 325 (2009) 1128–1131.
[5] G. Whitesides, The origins and the future of microfluidics, Nature 442 (2006) 368–373.
[6] S. Vyawahare, A.D. Griffiths, C.A. Merten, Miniaturization and parallelization of biological and chemical assays in microfluidic devices, Chem. Biol. 17 (2010) 1052–1065.
[7] J. El-Ali, P. Sorger, K. Jensen, Cells on chips, Nature 442 (2006) 403–411.
[8] R. Austin, C. Tung, G. Lambert, D. Liao, X. Gong, An introduction to micro-ecology patches, Chem. Soc. Rev. 39 (2010) 1049–1059.
[9] J. Knight, A. Vishwanath, J. Brody, R. Austin, Hydrodynamic focusing on a silicon chip: mixing nanoliters in microseconds, Phys. Rev. Lett. 80 (1998) 3863–3866.
[10] Q. Zhang, G. Lambert, D. Liao, H. Kim, K. Robin, C.-K. Tung, N. Pourmand, R.H. Austin, Acceleration of emergence of bacterial antibiotic resistance in connected microenvironments, Science 333 (2011) 1764–1767.
[11] K. Loutherback, J. Puchalla, R. Austin, J. Sturm, Deterministic microfluidic ratchet, Phys. Rev. Lett. 102 (2009) 45301.
[12] G. Lambert, D. Liao, R. Austin, Collective escape of chemotactic swimmers through microscopic ratchets, Phys. Rev. Lett. 104 (2010) 168102.

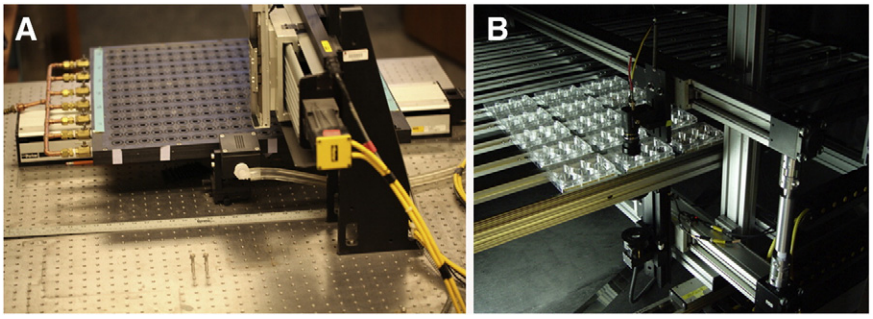

Fig. 7. (A) "Small" version of large scale massively parallel drug dosing array. Each circle is a separate vacuum hold-down for an individual array of micro-habitats; an epifluorescence camera head mounted by the x–y motorized stage can scan the entire array sequentially versus time. (B) Large array with nearly 10× the capacity that uses rails and linear actuators to move an imaging system from experiment to experiment.

[13] Q. Zhang, K. Robin, D. Liao, G. Lambert, R.H. Austin, The Goldilocks principle and antibiotic resistance in bacteria, Mol. Pharm. 8 (2011) 2063–2068.
[14] J. Hong, S. Quake, et al., Integrated nanoliter systems, Nat. Biotechnol. 21 (2003) 1179–1183.
[15] D. Mark, P. Weber, S. Lutz, M. Focke, R. Zengerle, F. von Stetten, Aliquoting on the centrifugal microfluidic platform based on centrifugo-pneumatic valves, Microfluid. Nanofluid. 10 (2011) 1279–1288.
[16] I. Araci, S. Quake, Microfluidic very large scale integration (MVLSI) with integrated micromechanical valves, Lab Chip 12 (2012) 2803–2806.
[17] J. Tsai, L. Lin, Active microfluidic mixer and gas bubble filter driven by thermal bubble micropump, Sensors Actuators A Phys. 97 (2002) 665–671.
[18] K. Kannappan, G. Bogle, J. Travas-Sejdic, D. Williams, Computational design of mixers and pumps for microfluidic systems, based on electrochemically-active conducting polymers, Phys. Chem. Chem. Phys. 13 (2011) 5450–5461.
[19] C. Lee, C. Chang, Y. Wang, L. Fu, Microfluidic mixing: a review, Int. J. Mol. Sci. 12 (2011) 3263–3287.
[20] O. Graydon, Microfluidics: laser-induced bubbles create valves and pumps, Nat. Photonics 5 (2011) 256.
[21] J. Kim, M. Kang, E. Jensen, R. Mathies, Lifting gate PDMS microvalves and pumps for microfluidic control, Anal. Chem. 84 (4) (2012) 2067–2071, http://dx.doi.org/10.1021/ac202934x.
[22] R. Gómez-Sjöberg, A.A. Leyrat, D.M. Pirone, C.S. Chen, S.R. Quake, Versatile, fully automated, microfluidic cell culture system, Anal. Chem. 79 (2007) 8557–8563.
[23] A. Groisman, C. Lobo, H. Cho, J.K. Campbell, Y.S. Dufour, A.M. Stevens, A. Levchenko, A microfluidic chemostat for experiments with bacterial and yeast cells, Nat. Methods 2 (2005) 685–689.
[24] E.W. Young, D.J. Beebe, Fundamentals of microfluidic cell culture in controlled microenvironments, Chem. Soc. Rev. 39 (2010) 1036–1048.
[25] P.J. Lee, T.A. Gaige, P.J. Hung, Dynamic cell culture: a microfluidic function generator for live cell microscopy, Lab Chip 9 (2009) 164–166.
[26] Q. Zhang, R.H. Austin, Applications of microfluidics in stem cell biology, BioNanoScience 2 (2012) 277–286.
[27] D. Huh, H.J. Kim, J.P. Fraser, D.E. Shea, M. Khan, A. Bahinski, G.A. Hamilton, D.E. Ingber, Microfabrication of human organs-on-chips, Nat. Protoc. 8 (2013) 2135–2157.
[28] C.Y. Chan, P.-H. Huang, F. Guo, X. Ding, V. Kapur, J.D. Mai, P.K. Yuen, T.J. Huang, Accelerating drug discovery via organs-on-chips, Lab Chip 13 (2013) 4697–4710.
[29] J.E. Barrick, R.E. Lenski, Genome dynamics during experimental evolution, Nat. Rev. Genet. 14 (2013) 827–839.
[30] E. Toprak, A. Veres, J.-B. Michel, R. Chait, D.L. Hartl, R. Kishony, Evolutionary paths to antibiotic resistance under dynamically sustained drug selection, Nat. Genet. 44 (2011) 101–105.
[31] M.M. Desai, D.S. Fisher, A.W. Murray, The speed of evolution and maintenance of variation in asexual populations, Curr. Biol. 17 (2007) 385–394.
[32] G.I. Lang, D.P. Rice, M.J. Hickman, E. Sodergren, G.M. Weinstock, D. Botstein, M.M. Desai, Pervasive genetic hitchhiking and clonal interference in forty evolving yeast populations, Nature 500 (2013) 571–574.
[33] S.-C. Park, J. Krug, Clonal interference in large populations, Proc. Natl. Acad. Sci. 104 (2007) 18135–18140.
[34] T.B. Kepler, A.S. Perelson, Drug concentration heterogeneity facilitates the evolution of drug resistance, Proc. Natl. Acad. Sci. 95 (1998) 11514–11519.
[35] B.B. Kaufmann, D.T. Hung, The fast track to multidrug resistance, Mol. Cell 37 (2010) 297–298.
[36] P.S. Dittrich, A. Manz, Lab-on-a-chip: microfluidics in drug discovery, Nat. Rev. Drug Discov. 5 (2006) 210–218.
[37] D. Lombardi, P.S. Dittrich, Advances in microfluidics for drug discovery, Expert Opin. Drug Discov. 5 (2010) 1081–1094.
[38] J.J. Agresti, E. Antipov, A.R. Abate, K. Ahn, A.C. Rowat, J.-C. Baret, M. Marquez, A.M. Klibanov, A.D. Griffiths, D.A. Weitz, Ultrahigh-throughput screening in drop-based microfluidics for directed evolution, Proc. Natl. Acad. Sci. 107 (2010) 4004–4009.
[39] Y. Ishida, Sewall Wright and Gustave Malecot on isolation by distance, Philos. Sci. 76 (2009) 784–796.
[40] Q. Zhang, R.H. Austin, Physics of cancer: the impact of heterogeneity, Ann. Rev. Condens. Matter Phys. 3 (2012) 363–382.
[41] E.A. Carlson, HJ Muller's contributions to mutation research, Mutat. Res. Rev. Mutat. Res. 752 (2013) 1–5.
[42] K. Drlica, X.L. Zhao, DNA gyrase, topoisomerase IV, and the 4-quinolones, Microbiol. Mol. Biol. Rev. 61 (1997) 377.
[43] S.M. Rosenberg, Evolving responsively: adaptive mutation, Nat. Rev. Genet. 2 (2001) 504–515.
[44] R.T. Cirz, J.K. Chin, D.R. Andes, V. de Crcy-Lagard, W.A. Craig, F.E. Romesberg, Inhibition of mutation and combating the evolution of antibiotic resistance, PLoS Biol. 3 (2005) e176.
[45] A. Khodursky, B. Peter, M. Schmid, J. DeRisi, D. Botstein, P. Brown, N. Cozzarelli, Analysis of topoisomerase function in bacterial replication fork movement: use of DNA microarrays, Proc. Natl. Acad. Sci. 97 (2000) 9419.
[46] S. Pestka, The use of inhibitors in studies on protein synthesis, Methods Enzymol. 30 (1974) 261–282.
[47] J. Davies, Inactivation of antibiotics and the dissemination of resistance genes, Science 264 (1994) 375–382.
[48] M. Krzywinski, J. Schein, İ. Birol, J. Connors, R. Gascoyne, D. Horsman, S. Jones, M. Marra, Circos: an information aesthetic for comparative genomics, Genome Res. 19 (2009) 1639–1645.
[49] P. Hastings, J. Lupski, S. Rosenberg, G. Ira, Mechanisms of change in gene copy number, Nat. Rev. Genet. 10 (2009) 551–564.
[50] K. Inoue, J. Lupski, Molecular mechanisms for genomic disorders, Annu. Rev. Genomics Hum. Genet. 3 (2002) 199–242.
[51] P. Wang, L. Robert, J. Pelletier, W.L. Dang, F. Taddei, A. Wright, S. Jun, Robust growth of *Escherichia coli*, Curr. Biol. 20 (2010) 1099–1103.
[52] S. Sawai, X.J. Guan, A. Kuspa, E.C. Cox, High-throughput analysis of spatio-temporal dynamics in *Dictyostelium*, Genome Biol. 8 (2007).
[53] L. Kim, Y.-C. Toh, J. Voldman, H. Yu, A practical guide to microfluidic perfusion culture of adherent mammalian cells, Lab Chip 7 (2007) 681–694.
[54] I. Meyvantsson, D.J. Beebe, Cell culture models in microfluidic systems, Annu. Rev. Anal. Chem. 1 (2008) 423–449.
[55] A. Wu, K. Loutherback, G. Lambert, L. Estévez-Salmerón, T.D. Tlsty, R.H. Austin, J.C. Sturm, Cell motility and drug gradients in the emergence of resistance to chemotherapy, Proc. Natl. Acad. Sci. 110 (2013) 16103–16108.
[56] H.J. Kim, D. Huh, G. Hamilton, D.E. Ingber, Human gut-on-a-chip inhabited by microbial flora that experiences intestinal peristalsis-like motions and flow, Lab Chip 12 (2012) 2165–2174.
[57] G. Lambert, L. Estévez-Salmeron, S. Oh, D. Liao, B.M. Emerson, T.D. Tlsty, R.H. Austin, An analogy between the evolution of drug resistance in bacterial communities and malignant tissues, Nat. Rev. Cancer 11 (2011) 375–382.